Dry heating treatment: A potential tool to improve the wheat starch properties for 3D food printing application

Bianca C. Maniglia, Dâmaris C. Lima, Manoel da Matta Júnior, Anthony Oge, Patricia Le-Bail, Pedro E.D. Augusto, Alain Le-Bail

Dry heating treatment: a potential tool to improve the wheat starch properties for 3D food printing application

Bianca C. MANIGLIA [a,b,c,d]*, Dâmaris C. LIMA[d], Manoel da MATTA JÚNIOR[d], Anthony OGE[a,c], Patricia LE-BAIL[b,c]; Pedro E. D. AUGUSTO [d,e], Alain LE-BAIL[a,c]*

[a] ONIRIS-GEPEA UMR CNRS 6144 Nantes - France
[b] BIA-INRAE UR 1268 Nantes – France
[c] SFR IBSM INRA CNRS 4202
[d] Department of Agri-food Industry, Food and Nutrition (LAN), Luiz de Queiroz, College of Agriculture (ESALQ), University of São Paulo (USP), Piracicaba, SP – Brazil
[e] Food and Nutrition Research Center (NAPAN), University of São Paulo (USP), São Paulo, SP, Brazil
*biancamaniglia@usp.br; alain.lebail@oniris-nantes.fr

Abstract

The futuristic technology of three-dimensional (3D) printing is an additive manufacturing that allows obtaining creative and personalized food products. In this context, the study of food formulations (named as "inks") to be processed through 3D printing is necessary. This work investigated the use of dry heating treatment (DHT), a simple and safe method, to improve the wheat starch properties aiming to produce hydrogels to be used as "inks" for 3D printing. Wheat starch was processed by dry heating for 2 (DHT_2h) and 4 h (DHT_4h) at 130 ºC. Modified wheat starches showed an increase in granule size, but processing did not alter the granule's shape nor surface, neither alter the molecular functional groups. On the other hand, DHT promoted slight molecular depolymerization, and reduction of starch crystallinity. Hydrogels "inks" based on the modified starches showed lower peak apparent viscosity during pasting, higher structural strength at rest, higher resistance to external stresses, higher gel firmness, and lower syneresis than hydrogels based on native starch. The hydrogels based on starch DHT_4h showed the best printability (greater ability to make a 3D-object by layer-by-layer deposition and to support its structure once printed) and this "ink" showed better reproducibility. Another point observed is that DHT extended the texture possibilities of printed samples based on wheat starch hydrogels. These results suggested that DHT is a relevant process to improve the properties of hydrogels based on wheat starch, making this ink suitable for 3D printing application.

Keywords: modified starch, 3D food printing, additive manufacturing, personalized food, food texture.

1. Introduction

The three-dimensional (3D) printing is an emerging technology to create personalized objects from digital models through the successive layer-by-layer deposition of materials such as plastic, metal, ceramics, or even living cells (Bhatia & Ramadurai, 2017). Currently, 3D printing technology has been used for food printing, defining new borders for food processing and being able to deliver a product that suits special consumer's criteria of taste, texture, cost, convenience and nutrition. For instance, 3D food printing can create unique novel textured foods, healthy foods, and smooth and easy-to-swallow foods for elderly people (Dankar, Haddarah, Omar, Sepulcre, & Pujola, 2018).

Extrusion is the most common 3D printing method for food applications, being relatively easy to develop and presenting different alternatives of "inks" (Guvendiren, Molde, Soares, & Kohn, 2016; Tan, Toh, Wong, & Lin, 2018). This process depends heavily on the physical properties of the material to be processed, which is one of the most important research topics about 3D printing (Liu, Liang, Saeed, Lan, & Qin, 2019). Therefore, it is important to study physicochemical and rheological aspects of possible "inks" used to print - in other words, their printability, i.e. their ability to make a 3D-object by layer-by-layer deposition, to obtain a defined shape and to support its structure once printed (Godoi, Prakash, & Bhandari, 2016).

In this context, it is important to study the ability of starch sources to be used as "inks". As one of the most important carbohydrates in human diets and one of the most available in nature, starch is widely used as thickening and gelling agents in many food formulations (BeMiller, 2011). The gelatinized starch paste shows a shear-thinning behavior and instant responses to the applied shear strains, being easily extruded from the fine nozzle (Evans & Haisman, 1980; Le Tohic et al., 2018). Finally, the starch hydrogel can present good printability, depending on the sources and modification processes.

In fact, some studies have already explored starchy products as "inks" for 3D printing, like potato starch (Yang, Zhanga, & Bhandari, 2018), mashed potatoes (Liu et al., 2018), potato puree (Dankar et al., 2018), wheat flour (Liu, Liang, Saeed, Lan, & Qin, 2019a), rice flour (Anukiruthika, Moses, & Anandharamakrishnan, 2020). Moreover, our group has evaluated some alternatives to modify starches and improve the 3D printability, such as the ozone and dry heating treatment of cassava starch (Maniglia et al. (2019) and Maniglia et al. (2020)). However, the approach of starch modification for 3D printing application is still under-explored in the literature, considering different sources and modification technologies.

Wheat starch is the third most-produced starch in the world, being a coproduct in the vital gluten industry (Shevkani, Singh, Bajaj, & Kaur, 2017). It has an important role in many food products (Agama-Acevedo, Flores-Silva, & Bello-Perez, 2019; Ubeyitogullari & Ciftci, 2016), being frequently used in gluten-free baked products (Houben, Höchstötter, & Becker, 2012). However, native wheat starch produces weak-bodied, cohesive, rubbery pastes when heated and undesirable gels when the pastes are cooled (Punia, Sandhu, Dhull, & Kaur, 2019).

In this way, modification processes can be used to improve wheat starch properties and applicability. Among different possibilities, dry heat treatment (DHT) is a simple physical method, considered a "green" technology (chemical-free, simple, safe and pollution-free) to alter starch structure and functionality (Chandanasree, Gul, & Riar, 2016; Gou et al., 2019; K. Liu, Hao, Chen, & Gao, 2019; Maniglia, Castanha, Le-Bail, Le-Bail, & Augusto, 2020; Oh, Bae, & Lee, 2018). Moreover, Maniglia et al. (2020) described that cassava starch DHT resulted in stronger gels with better 3D printability than the native starch. It is worth mention each starch source reacts differently to each modification technology, justifying the present work.

Wheat starch modification by DHT has scarcely been reported in the literature, although some studies are available with wheat flour (Nakamura, Koshikawa, & Seguchi, 2008; Ozawa, Kato, & Seguchi, 2009; Seguchi, 2001) – where the observed changes are mainly associated to the proteins.

Based on this context, this study aimed to use the DHT as a tool to improve the 3D printability of "inks" based on wheat starch hydrogels. To achieve it, firstly the effect of DHT was studied in relation to the wheat starch structure and properties. Then, the potential for 3D printing application was evaluated. The innovation of this study involves developing functional ingredients to be used as gelling and thickening agents to bring better printability for food products, also expanding the application and potential of wheat starch.

2. Material and methods

2.1 Material and dry heating treatment (DHT)

Native wheat starch (moisture content: 10.1 g/100 g) was purchased from Merck KGaA (Germany). All the chemicals were of analytical grade.

The dry heating treatment (DHT) was based on the work of Chandanasree et al. (2016). Wheat starch (50 g) was distributed evenly in a thin layer (~ 1 mm) and packaged on aluminum foil, as an envelope (30 x 20 cm), which was closed with a high-temperature tape to avoid moisture loss. The envelope was then placed in a hot-air convective oven (XU032,

Frances Etuves, Chelles, France) with air at 130 °C and 1 ± 0.1 m. s^{-1} for 2 and 4 h (named DHT_2h and DHT_4h, respectively).

The temperature was recorded using a datalogger with six K-type thermocouples (AOIP Datalog, Ris-Orangis, France) of 0.5 mm diameter for measuring the temperature in different locations within the sample (Supplementary Fig. S1A). The treatment time was counted from the moment where all parts of the envelope reached the processing temperature (130 °C) - the heat-up time was 20 min (Supplementary Fig. S1B). After processing, the starch was cooled, sieved (250 µm), and stored in glass containers for further analysis.

2.2 Granule characterization: morphology and size distribution

The starch granules morphology (control and modified) was observed using a light microscope (model L1000, Bioval, Curitiba, Brazil; with a 20 W halogen lamp, the magnification of 40 x) and a digital camera of 5.1 megapixels (MT9P001, Aptina, Colorado, USA). The starch granules were dispersed in distilled water (1:1, v/v). Then, they were placed on a glass slide, covered by a glass coverslip, and directly evaluated. A polarized light filter coupled to the system was used to observe the Maltese crosses.

The granule size distribution was determined using the dynamic light scattering (DLS) of Malvern Master Size (3000, Malvern Instruments Ltd, Worcestershire, UK). The samples were dispersed in the air. The analyse was carried out 4 times for each sample. From the obtained data, the volume-based mean (D[4,3]) and the area-based mean (D[3,2]) diameters were calculated. The diameters d(0.1), d(0.5), and d(0.9) were also obtained, describing the dimension that 10 %, 50 %, and 90 % of the granules were smaller, respectively.

2.3 Molecular characterization: pH, functional groups, molecular size distribution

pH values were measured in the starch suspension of 10.7% (w/w) in distilled water, under constant stirring at room temperature (25 °C), using a potentiometer (model TEC-5 mode, Tecnal, Piracicaba, Brazil).

The carboxyl and carbonyl contents were determined by the method of Smith (1967) and Chattopadhyay, Singhal, & Kulkarni (1997), respectively, with some modifications, as described by Maniglia et al. (2020). Their content was expressed as the number of carboxyl (COOH / 100 GU) or carbonyl (CO/100 GU) groups in relation to 100 units of glucose. The analyses were done in triplicate.

The changes in the functional groups were also evaluated using the infrared spectroscopy technique. Fourier transform infrared (FTIR) spectroscopy was conducted using a Spectrum 100™ FTIR instrument (Perkin-Elmer, Shelton, USA) equipped with an attenuated total reflection (ATR) accessory. All the spectra were the average of 16 scans from 4000 cm^{-1} to 650 cm^{-1} and were acquired at a resolution of 4 cm^{-1}.

The molecular size distribution profile (control, DHT_2h, and DHT_4h) was determined using a gel permeation chromatography (GPC) system, according to Song & Jane (2000), with some modifications described by Maniglia, Lima, Junior, et al. (2019).

2.4 Thermal and crystalline properties of starch

The thermal properties during starch gelatinization were determined using a Multi-Cell Differential Scanning Calorimeter (MC-DSC) – (TA Instruments, Lindon, USA). The starch samples were weighed and hydrated directly into the ampoules (10 g dry starch / 100 g suspension). An ampoule with deionized water was used as a reference and three runs for each sample were analysed. The MC-DSC heating program consisted of going from 20 to 120 °C at a rate of 2 °C/min. The onset temperature (To), the peak temperature (Tp), the conclusion temperature (Tc), and the enthalpy (ΔH) associated with the starch gelatinization interval were calculated with the aid of the Universal Analyzer software (TA Instruments, New Castle, USA).

The crystallinity of starch samples was determined by X-ray diffraction (XRD). Before the XRD analysis, the starch samples were maintained in a desiccator containing a saturated $BaCl_2$ solution (25 °C, a_w = 0.900) for 7 days to ensure constant water activity. The sample was examined by X-ray diffraction equipment Inel X-ray equipment (Inel, Centre-Val de Loire, France) operated at 40 kV and 30 mA. The CuKα radiation (0.15405 nm) was selected using a quartz monochromator. Diffracted intensities were monitored (2θ) by a sensitive detector (CPS 120, Inel, Centre-Val de Loire, France). The resulting diffraction diagrams were normalized between 3 and 30 ° (2θ). The curves obtained were smoothed using the Origin software, version 2018 (Microcal Inc., Northampton, USA). The relative crystallinity was calculated as the ratio of upper diffraction peak area to the total diffraction area, following the method described by Nara & Komiya (1983) and considering 2θ ranging from 3 to 30 °.

2.5 Starch pasting behaviour and hydrogel properties (rheology and firmness)

Starch pasting properties were determined using a Rapid Visco Analyzer (RVA4, Newport Scientific Pvt. Ltd., Warriewood, Australia) with Thermocline for Windows software, version 3.0. The RVA analysis consisted of heating, retention, and cooling cycle under constant shear (160 rpm). Following the standard conditions for starch characterization, starch suspensions of 10.7 g starch / 100 g (correct to 14 % moisture basis) were prepared for the RVA analyses. The procedure used was: keep at 50 ^{o}C for 1 min, then heat up to 95 ^{o}C (6 ^{o}C.min^{-1} and maintained 5 min), followed by cooling to 50 ^{o}C (6 ^{o}C.min^{-1}), and finally, maintained at 50 ^{o}C for 2 min.

Different parameters are obtained to describe the pasting behaviour: peak apparent viscosity – PAV (the maximum paste apparent viscosity achieved in the heating stage), through apparent viscosity – TAV (minimum paste apparent viscosity achieved after holding at the maximum temperature), final apparent viscosity – FAV (the apparent viscosity at end of run), breakdown – BD (difference between PAV and TAV), setback – SB (the difference between FAV and PAV), and pasting temperature – PT (the temperature at which starch granules begin to swell and gelatinize due to water uptake). For a better interpretation of these parameters, the relative breakdown (RBD) and relative setback (RSB) were also calculated, following the study of Castanha, Matta Junior, & Augusto (2017). The RBD (calculated as the ratio between the BD and PAV values) can be associated with the facility of starch granules to disrupt, while the RSB (calculated as the ratio between the SB and TAV values) can be associated to the retrogradation tendency.

Hydrogels were prepared by dispersing starch in distilled water (10.7 g dry starch/ 100 g, being the starch mass corrected to 14 % moisture basis), and then heating it at 85 ± 2 °C in glass containers in a water bath for 20 min. Then, the pastes were placed in plastic cups (40 mm diameter × 20 mm height) and stored for 24 h in the refrigerator (5 ± 2 °C) to gelling. The cups were kept in a desiccator with water at the bottom to ensure uniform moisture. The obtained hydrogels were evaluated in relation to their viscoelasticity and firmness behaviours.

The viscoelastic properties were analysed by oscillatory stress sweep using a HAAKE MARS rheometer (Vane FL40, ThermoFisher, Karlsruhe, Germany). The hydrogels were loaded between the stainless steel parallel plates geometry (with a diameter of 25 mm and a gap of 1 mm), trimmed, and their edge was covered with silicon oil to prevent water vaporization. The stress sweep measurements were carried out at 22 ^{o}C with a logarithmically increasing shear stress at a frequency of 0.1 Hz (initial stress 0.001 Pa). This analysis was conducted in triplicate.

The hydrogel firmness was determined by a puncture assay using a texture analyzer TA TX Plus (Stable Micro Systems Ltd., Surrey, UK) with a load cell of 50 kgf (490.3 N). The samples were removed from the refrigerator and analysed immediately to ensure a constant temperature. The samples were penetrated until a distance of 4 mm using a cylindrical probe (P/0.5R, 0.5 in of diameter) at 1 mm·s^{-1}. The equipment measured the force as a function of penetration depth. Gel firmness was evaluated by the energy required to penetrate the material (calculated by the area below the curve force versus distance of penetration). This analysis was conducted in triplicate.

2.6 Syneresis measurement

Syneresis was determined according to the method of Yeh & Yeh (1992). Briefly, starch suspensions (5 % w/w) were gelatinized at 85 °C for 20 min in a temperature-controlled water bath followed by cooling to room temperature. The pastes were then stored for 24 h at 4 °C. Syneresis was measured gravimetrically as the amount of water (g water/ 100 g gel) released after centrifugation at 1500 g for 15 min. Triplicate of the results were read and the mean reported.

2.7 3D printing process

The "inks" (starch hydrogels) were prepared identically as described on the last section. After heating, the hydrogels were transferred for the printer syringes (60 mL), cooled to room temperature to form a weak gel-like structure, and stored in the refrigerator (5 ± 2 °C) for 24 h before the printing.

The printing process was carried out in a 3D printer (Stampante 3DRAG V1.2, Futura Elettronica, Gallarate, Italy) presented in Fig. 1. The syringes with the hydrogels were removed from the refrigerator and immediately positioned in the 3D printer. A nozzle with diameter of 0.8 mm and height of 18 mm was coupled in the syringes. The 3D printing conditions were: nozzle movement of 5 mm/s and an extrusion rate of 4.5 mg/s at 20 ºC.

Three physical models (heart, star, and cylinder shapes) were created using the Repetier Host V2.0.1 and Slic3r software (Hot-World GmbH & Co. KG, Willich, Germany). The dimensions of the cylinder shape were 2 cm x 4 cm (diameter × height), for the star shape were 2.5 cm × 2.5 cm × 2 mm (Length × Width × Height), and for the heart shape were 5 cm × 6 cm × 2 mm (Length × Width × Height). 5 samples were printed for each hydrogel and

shape. All the printing experiments were carried out at room temperature. After printing, the samples were photographed.

The reproducibility of the 3D printed samples was evaluated considering the weigh and the dimensions of the sample printed. Each printed cylinder was weighed in analytical balance (AZ214, Sartorius, Göttingen, Germany) and their dimensions (height and diameter) were measured in five different positions using a digital paquimeter (CD-6 CSX-B model, Mitutoyo, Roissy-en-France, France).

Printed samples in cylinder shape were conditioned in a refrigerator (at 5 ± 2 °C) for 24 h, inside of a desiccator with water to avoid dehydration. Then, these printed samples were used for texture analysis.

2.8 Texture profile of the printed hydrogels

A texture analyser TA-XT+ (Stable Microsystems, Surrey, UK) was used to assess the printed cylinders. These analyses were conducted immediately in the samples removed from the refrigerator in triplicates for each sample.

The texture profile analysis (TPA) measurement consisted of two compression-decompression cycles separated by a time interval of 10 s, at a rate of 1 mm/s, using a cylindric probe (25 mm diameter, Code P/25, Stable Micro System Ltd., Surrey, UK). The probe compressed the sample to 25 % (6.25 mm) of the initial height (25 mm) before decompression using a 50 kgf (490.3 N) load cell.

All the textural parameters were measured and calculated by the instrument software from the resulting force-deformation curves, including hardness, adhesiveness, cohesiveness, springiness, gumminess, and chewiness.

2.9 Experimental design and Statistical analysis

A completely randomized design was conducted. All processes and analyses were carried out at least in triplicate. To evaluate differences, analysis of variance (ANOVA) and Tukey's test at a 5 % significance level were accomplished by using the software *Statistic 13* (StatSoft, USA).

3. Results and Discussion

3.1 Starch granule: size distribution and morphology

Fig. 2 shows the granule size distribution (A) and specific diameters (B) for the control and modified wheat starch. The samples displayed a unimodal size distribution and DHT resulted in larger granules sizes (Fig. 2A), being this effect consistent with the duration of the dry heating process: the D[4,3] varied from 21.7 µm for the control starch to 22.6 and 24.1 µm for DHT_2h and DHT_4h, respectively (Fig. 2B). The same was observed for the D[3,2], varied from 13.3 µm for the control starch to 13.7 and 14.1 µm for DHT_2h and DHT_4h, respectively (Fig. 2B). Since the parameter D[4,3] is more sensitive to larger granules, while D[3,2] is more sensitive to the fraction of smaller granules (Lopez-Sanchez et al., 2011), it is noted that the greatest effect of the DHT occurred for the larger granules. This behavior is similar to that observed for cassava starch treated with DHT (Maniglia et al., 2020). It can be associated with a possible expansion in the starch granule due to water vaporization, such as during flash vaporization. In fact, part of the water content in the samples was vaporized during DHT, as reflected by the moisture of modified wheat starches (control: 10.1 g/100 g; DHT_2h: 4.7 g/100 g and DHT_4h: 4.5 g/100 g). The dry heating process also increased the number of granules with bigger sizes considering the d0.1, d0.5, and d0.9 values.

Fig. 3 shows the optical microscopy of the control and treated wheat starches using both nonpolarized and polarized light. The microscopies show wheat starch granules with lenticular morphology with a large variety of granules size, which is consistent with previous observation (Hruska, Arevao, Muñoz, & Avila, 2019).While the birefringence effect (Maltese cross is visible) can be seen in all the images, the processed samples showed a shine reduction. Chung, Liu, & Hoover (2010) attributed this behavior to the temperature elevation at the center of the starch granule, which supposedly damage the amylopectin double helices structure. The same behavior was observed by Liu et al. (2019) in the case of dry heating treatment for waxy potato starch. Once the Maltese crosses still can be seen, it indicates the thermal energy provided was not sufficient to destroy amylopectin double helices structure.

These results indicated that DHT did not alter the shape nor altered the granules surface; however, it slightly affected the internal microstructure of wheat starch granules and promoted an expansion of the granule size – which can affect starch properties.

293 ***3.2 Starch molecular properties***

294 DHT processing did not change the pH of the wheat starches suspensions (control:
295 5.90 ± 0.10, DHT_2h: 6.06 ± 0.15, and DHT_4h: 5.98 ± 0.18), and no carbonyl and carboxyl
296 formation was found. It indicates that DHT did not promote starch oxidation. It is interesting
297 to observe that cassava starch, at the same processing conditions, presented carbonyl groups
298 formation (Maniglia et al., 2020), highlighting each starch source are differently affect by
299 processing.

300 Fig. 4(A) shows the vibrational spectra of the control and modified starches. All
301 samples showed the same characteristic bands at 3323 cm^{-1}, 2934 cm^{-1}, 1648 cm^{-1}, 1339
302 cm^{-1}, 1150 cm^{-1}, 1020 cm^{-1}, and 996 cm^{-1}. The bands at 3500 and 2900 cm^{-1} are associated
303 with OH bonds and CH_2 deformation, respectively (Kačuráková & Mathlouthi, 1996). Bands
304 at 1650 cm^{-1} are associated with water molecules absorbed in the amorphous region (Kizil,
305 Irudayaraj, & Seetharaman, 2002) and the stretching vibration of the CO band (amide I). The
306 peak at 1339 cm^{-1} can be associated to OH bending due to the primary or secondary alcohols
307 (Muscat, Adhikari, Adhikari, & Chaudhary, 2012). The fingerprint region of starch is the
308 bands at 1200-900 cm^{-1} (showed in Fig. 4(B)) and this region provided information about
309 changes in the polymeric structure and conformation of starch (Dankar et al., 2018). The
310 intense IR band at 996 cm^{-1} can be mainly attributed to skeletal mode vibrations of α $1 \rightarrow 4$
311 skeletal glycoside bonds (Jao & Ko, 2002). In addition, the middle strong peaks at 1150 cm^{-1}
312 and 1060 cm^{-1} are mainly attributed to the stretching vibration of CO and bending vibration
313 of C-O-H (Hou et al., 2019). The band at 1060 cm^{-1} has been linked to amorphous structures
314 (Xiong, Li, Shi, & Ye, 2017). On the other hand, the band at 996 cm^{-1} can be associated with
315 the single helix crystalline related to hydrogen bonds of anhydroglucose unit (Xiong et al.,
316 2017).

317 It was not observed a significant difference between the presence and intensity of the
318 bands in control and modified starches. These results indicate and confirm that the dry heating
319 treatment did not modify the functional groups.

320 Fig. 5 shows the molecular size distribution of the control and treated wheat starches.
321 The first peak consists of molecules of larger size and more ramifications, which can be
322 associated with amylopectins, while the second peak represents molecules of smaller size and
323 a linear structure, which can be associated with amyloses. DHT reduced the molecular size
324 (Fig. 5): the first peak was slightly reduced, the fraction of molecules with intermediary size
325 was also reduced, and the second peak was increased; moreover, the first and second peaks

scrolled to the right. It indicates the DHT promoted the formation of molecules with lower size (which are retained longer in the chromatographic column) due to depolymerization promoted by cleavage of glycosidic linkages. The depolymerization affected mainly the intermediate size molecules. Maniglia et al. (2020) also observed this behaviour for cassava starch, although with a much more accentuated effect. These results are also consistent with the study of Lei et al. (2020) involving maize starch. The authors observed the temperature increasing of DHT reduced drastically the long-amylose chains, while more short-amylose chains were formed.

The molecular results reinforce each starch source are differently affect by processing. Consequently, further structure and properties evaluations are needed.

3.3 Thermal and crystalline properties of starch

The differential scanning calorimetry (DSC) thermograms (A) and the X-ray diffractograms (B) of the control and modified wheat starches are shown in Fig. 6. The gelatinization properties were obtained (Table 1) from Fig. 6(A). There was no difference in the onset (To) and the final (Tf) temperatures among treatments. The peak temperature (Tp) increased significantly ($p < 0.05$) as the treatment period increased, and the gelatinization enthalpy (ΔH) was reduced ($p < 0.05$) only for the DHT_4h starch. Lei et al. (2020) also observed a reduction of the gelatinization enthalpy (ΔH) for maize starch treated by DHT.

The enthalpy of gelatinization is an indirect measure of the amount of starch crystalline region (or double helices structure) which are broken during heating (Liu, Yu, Xie, & Chen, 2006). Therefore, ΔH reduction can indicates the formation of weaker structures, which were less crystalline. In fact, Fig. 6(B) show the typical A-type diffraction pattern of wheat starch, with two singlet peaks (2θ) at 15° and 22.8°, a doublet peak (2θ) at 16.8° and 17.8°, and two weak peaks (2θ) at 5.6° and 20°. In addition, Fig. 6(B) shows the relative crystallinity of DHT_4h was lower than control and DHT_2h starches. Therefore, the XRD results are consistent with the DSC results, indicating that DHT reduced the double-helical crystals and decreased the order of starch crystalline structure – as also observed by (Lei et al., 2020).

The thermal and crystalline results are consistent with the behavior observed by optical microscopy about the reduction of Maltese crosses brightness in modified starches. All these results pointed out that the DHT reduced the crystalline zones of wheat starch. Even so, the starch properties must be evaluated.

3.4 Starch pasting properties

Fig. 7 (A) shows the RVA curves for control and wheat starch treated by DHT. Table 2 shows the pasting parameters obtained from RVA and the parameters.

The dry heating treatment significantly ($p < 0.05$) decreased the peak apparent viscosity (PAV), and there was a greater effect on this parameter as treatment time increased. This effect can be associated with cleavage of glycosidic linkages which resulted in weakening of starch granules resulting in minor capacity to maintain the granule integrity (Chung, Min, Kim, & Lim, 2007).

The pasting temperature (PT) is the temperature at which starch granules begin to swell due to water uptake (Gałkowska & Juszczak, 2019). DHT applied for 4 h slightly increased PT, which can be related with the presence of a greater fraction of small-sized molecules, that require more energy to gelatinize than large-size molecules similar to that observed by Lima et al., (2020).

Moreover, as the dry heating treatment period increased, a significant reduction ($p < 0.05$) of the through apparent viscosity (TAV) and final apparent viscosity (FAV) occurred. It can be associated with the thermal degradation of crystalline structures (observed in DSC and XRD analysis) and depolymerization (cleavage of glycosidic linkages) promoted by DHT (Zou, Xu, Tian, & Li, 2019).

The increase of the DHT period also increased the RBD and reduced the RSB parameters, when compared to control starch (data shown in Table 2), indicating that the granules are more fragile, more susceptible to rupture, and less prone to re-associate. According to Castanha et al. (2017), this behavior can be attributed to the change in the molecular size distribution.

Therefore, pasting properties confirm the structural modifications due to DHT processing, as well as they indicate hydrogels can present unique properties.

3.5 Hydrogel properties: rheology, firmness, and syneresis

Fig. 7 shows the results of (B) oscillatory stress sweep analysis, (C) gel firmness, and (D) the energy required in a puncture assay, considering the control and the wheat starch modified by DHT (2 and 4 h). Table 2 shows the parameters obtained from oscillatory stress sweep analysis.

Fig. 7(B) shows the representative storage (G') and loss (G'') modulus curves: the G' in this plateau region is a measure of the elasticity of material at very small deformation and it can be taken as a measure of the structural strength of mechanical rigidity of material at rest (Lille, Nurmela, Nordlund, Metsä-Kortelainen, & Sozer, 2018; Mezger, 2006). Moreover, for both control and modified starches, G' > G'' which indicates that all samples show a solid/elasticity dominating gel-like structure. G' increased with the DHT period, as well as the ration G'/G'', which indicates this treatment promoted the formation of a gel with greater rigidity and capacity to recover the shape after suffering stress. Therefore, this hydrogel probably shows good properties to be printed, because it can recover better the shape when it is deposited on the surface – being this evaluated in the next section.

The yield stress ($\sigma_{0,G'}$) is the stress where G' starts to decrease after the plateau region (Table 2), which indicates the stress at which the network/structure of the material starts to break down. The $\sigma_{0,G'}$ can be related to the ability of the material to keep its shape under gravity and the stresses generated by material layers deposited on top of it (Lille et al. 2018). The $\sigma_{0,G'}$ value was greater as the DHT period increases. According to Lille et al. (2018), a material with high structural strength at rest (G′) and a certain degree of resistance to external stresses ($\sigma_{0,G'}$) is required to ensure good printability of a material. In this way, we can observe that the DHT improved these rheological parameters of the wheat starch hydrogel, indicating that it can be a better material to be used in 3D printing.

Fig. 7(C) and 7(D) show the gels produced with modified starches showed higher firmness than the control, and this behavior was more accentuated as the treatment period increased. The molecular depolymerization promoted by DHT (Fig. 5) probably resulted in size distribution that better re-associate and packing, forming a stronger three-dimensional network structure. In this way, DHT promoted the formation of stronger gels, expanding the industrial applications of wheat starch.

During starch gels cooling, molecular retrogradation and amylose tendency to crystallize releases water from the gels – which is called synereis. The syneresis prejudices the printability of the hydrogels, as well as the consumer perception. DHT reduced syneresis, which is an interesting result: control: 7.38 ± 0.71 g water/ 100 g gel, DHT_2h: 5.19 ± 0.19 g water/ 100 g gel, DHT_4h: 3.62 ± 0.13 g water/ 100 g gel). As a result, these "inks" appeared well adapted to 3D printing use - in fact, this behavior can be seen in Fig. 8. Pictures of the syneresis in the hydrogels are shown in the Supplementary Fig. S2.

3.6 3D printing performance and characterization

Fig. 8 shows the star, heart, and cylinder shaped structures, printed using the hydrogels based on control and modified starches as "inks". Overall, the printed samples in our work were very similar to the pre-designed virtual model, indicating that the 3D printing could achieve precise printing with a personalized design using wheat hydrogels. All hydrogels could be smoothly extruded from the nozzle. However, the hydrogel based on control starch showed a scattering on the surface and a syneresis effect (visible in the star shape, which is consistent with the results presented in Section 3.4). The modified starches showed higher gel consistency, without spreading on the surface. The hydrogel based on DHT_4h starch showed the best resolution with the lines having higher cohesiveness and being more continuous. The behavior of the hydrogels after 3D printing can be associated with the rheological parameters: the hydrogels with higher G´ and $\sigma_{0,G'}$ showed the best printability.

Texture is an important sensory attribute of food acceptability (Yu, Ren, Zhao, Cui, & Liu, 2020). In this way, the printed cylinders were evaluated in relation to its textural parameters (Table 3). Results showed there was no significant difference in the cohesiveness, springiness, and chewiness values of printed samples. On the other hand, the increase of the heating period caused a significant ($p<0.05$) increase on hardness. According to Yang, Zhang, Prakash, & Liu (2018b), higher G′ indicates stronger mechanical strength often accompanied by greater hardness, behavior also observed in our results. The modified starches resulted in printed samples with less adhesiveness. According to Anukiruthika, Moses, & Anandharamakrishnan (2020), less adhesive "inks" flow more easily through the nozzle, contributing to the 3D printing process. In this way, DHT extended the possibility of textures of printed samples based on wheat starch hydrogels.

About reproducibility, the hydrogels based on modified starches showed lower weight and higher height than hydrogel based on control starch. The diameter did not show a significant difference among the treatments. Moreover, by comparing the standard deviation, we observed lower values for DHT_4h, indicating this treatment formed hydrogel were more reproducible 3D printing.

Finally, comparing this study with the previous of our group (Maniglia et al., 2020), we can observe that the same physical modification, DHT, showed different effects for each starch source, affecting the final printability characteristic. The modified cassava starch was more depolymerized, suffered oxidation, and showed gel firmness much higher than the

native one, when compared with the changes here reported for wheat starch. Modified wheat starch showed a reduction in syneresis, which is important for 3D printing application. In this way, our results provide information on the benefits DHT modification can bring to each source, mainly focusing on the application of 3D printing.

4. Conclusion

This work investigated the use of dry heating treatment (DHT) as a tool to improve the printability of hydrogels ("inks") based on wheat starch. DHT caused a slightly expansion of granule size; however, it did not alter the shape of the starch granules nor their surface. DHT did not change the functional groups of the starch, indicating a negligible oxidation. However, slight depolymerization of starch was observed, in special in the middle size molecules, as well as a reduction of the crystalline zones in starch granule. The hydrogels based on the modified starches showed lower apparent viscosity during pasting and greater structural strength at rest. The longer duration of DHT processing, higher was the firmness of the hydrogels, and more reduced was the syneresis. The changes promoted by DHT in wheat starch, in special in 4 h treatment, resulted in hydrogels with better printability and reproducibility in 3D printing.

In this study, we demonstrated that the DHT is a simple alternative to improve the properties of wheat starch, as well as extend the texture possibilities of printed samples based on wheat starch hydrogels. Finally, this study shows the possibilities to expand the potential application of this starchy source.

Declaration of Conflict of Interest

The authors declare no conflict of interest.

Acknowledgments

The authors are grateful to:

- the Région Pays de la Loire (France) / RFI "FOOD 4 TOMORROW" for funding the Post-doctoral fellowship "STARCH-3D" of BC Maniglia;
- the São Paulo Research Foundation (FAPESP, Brazil) for funding project n° 2019/05043-6;
- the National Council for Scientific and Technological Development (CNPq, Brazil) for funding the productivity grant of PED Augusto (306557/2017-7);

- this study was financed in part by the “Coordenação de Aperfeiçoamento de Pessoal de Nível Superior - Brazil (CAPES)” - Finance Code 001, through the DC Lima Ph.D. scholarship.

7. References

Agama-Acevedo, E., Flores-Silva, P. C., & Bello-Perez, L. A. (2019). Cereal Starch Production for Food Applications. In *Starches for Food Application* (pp. 71–102). Elsevier.

Anukiruthika, T., Moses, J. A., & Anandharamakrishnan, C. (2020). 3D printing of egg yolk and white with rice flour blends. *Journal of Food Engineering*, *265*, 109691.

BeMiller, J. N. (2011). Pasting, paste, and gel properties of starch–hydrocolloid combinations. *Carbohydrate Polymers*, *86*(2), 386–423.

Bhatia, S. K., & Ramadurai, K. W. (2017). 3D printing and bio-based materials in global health. *SpringerBriefs in Materials. Google Scholar*.

Castanha, N., Matta Junior, M. D. da, & Augusto, P. E. D. (2017). Potato starch modification using the ozone technology. *Food Hydrocolloids*, *66*, 343–356. https://doi.org/10.1016/j.foodhyd.2016.12.001

Chandanasree, D., Gul, K., & Riar, C. S. (2016). Effect of hydrocolloids and dry heat modification on physicochemical, thermal, pasting and morphological characteristics of cassava (Manihot esculenta) starch. *Food Hydrocolloids*, *52*, 175–182. https://doi.org/10.1016/j.foodhyd.2015.06.024

Chattopadhyay, S., Singhal, R. S., & Kulkarni, P. R. (1997). Optimisation of conditions of synthesis of oxidised starch from corn and amaranth for use in film-forming applications. *Carbohydrate Polymers*, *34*(4), 203–212. https://doi.org/10.1016/S0144-8617(97)87306-7

Chung, H.-J., Liu, Q., & Hoover, R. (2010). Effect of single and dual hydrothermal treatments on the crystalline structure, thermal properties, and nutritional fractions of pea, lentil, and navy bean starches. *Food Research International*, *43*(2), 501–508. https://doi.org/10.1016/j.foodres.2009.07.030

Chung, H.-J., Min, D., Kim, J.-Y., & Lim, S.-T. (2007). Effect of minor addition of xanthan on cross-linking of rice starches by dry heating with phosphate salts. *Journal of Applied Polymer Science*, *105*(4), 2280–2286. https://doi.org/10.1002/app.26237

Dankar, I., Haddarah, A., Omar, F. E. L., Sepulcre, F., & Pujola, M. (2018). 3D printing technology: The new era for food customization and elaboration. *Trends in Food Science*

521 *& Technology*, *75*, 231–242.
522 Evans, I. D., & Haisman, D. R. (1980). Rheology of gelatinised starch suspensions. *Journal of*
523 *Texture Studies*, *10*(4), 347–370.
524 Fanli Yang, Min Zhanga, Bhesh Bhandari, Y. L. (2018). Investigation on lemon juice gel as
525 food material for 3D printing and optimization of printing parameters. *LWT - Food*
526 *Science and Technology*, *87*, 67–76. https://doi.org/10.1016/j.lwt.2017.08.054
527 Gałkowska, D., & Juszczak, L. (2019). Effects of amino acids on gelatinization, pasting and
528 rheological properties of modified potato starches. *Food Hydrocolloids*, *92*, 143–154.
529 Godoi, F. C., Prakash, S., & Bhandari, B. R. (2016). 3d printing technologies applied for food
530 design: Status and prospects. *Journal of Food Engineering*, *179*, 44–54.
531 https://doi.org/10.1016/j.jfoodeng.2016.01.025
532 Gou, M., Wu, H., Saleh, A. S. M., Jing, L., Liu, Y., Zhao, K., … Li, W. (2019). Effects of
533 repeated and continuous dry heat treatments on properties of sweet potato starch.
534 *International Journal of Biological Macromolecules*, *129*, 869–877.
535 https://doi.org/10.1016/j.ijbiomac.2019.01.225
536 Guvendiren, M., Molde, J., Soares, R. M. D., & Kohn, J. (2016). Designing biomaterials for
537 3D printing. *ACS Biomaterials Science & Engineering*, *2*(10), 1679–1693.
538 Hou, S.-W., Wei, W., Wang, Y., Gan, J.-H., Lu, Y., Tao, N.-P., … Xu, C.-H. (2019).
539 Integrated recognition and quantitative detection of starch in surimi by infrared
540 spectroscopy and spectroscopic imaging. *Spectrochimica Acta Part A: Molecular and*
541 *Biomolecular Spectroscopy*, *215*, 1–8.
542 Houben, A., Höchstötter, A., & Becker, T. (2012). Possibilities to increase the quality in
543 gluten-free bread production: an overview. *European Food Research and Technology*,
544 *235*(2), 195–208.
545 Hruska, J. S., Arevao, S., Muñoz, F., & Avila, A. (2019). Impedance characterization of
546 wheat starch at various water contents. *Powder Technology*, *346*, 425–432.
547 Jao, C.-L., & Ko, W.-C. (2002). 1, 1-Diphenyl-2-picrylhydrazyl (DPPH) radical scavenging
548 by protein hydrolyzates from tuna cooking juice. *Fisheries Science*, *68*(2), 430–435.
549 Kačuráková, M., & Mathlouthi, M. (1996). FTIR and laser-Raman spectra of oligosaccharides
550 in water: characterization of the glycosidic bond. *Carbohydrate Research*, *284*(2), 145–
551 157.
552 Kizil, R., Irudayaraj, J., & Seetharaman, K. (2002). Characterization of irradiated starches by
553 using FT-Raman and FTIR spectroscopy. *Journal of Agricultural and Food Chemistry*,
554 *50*(14), 3912–3918.

555 Le Tohic, C., O'Sullivan, J. J., Drapala, K. P., Chartrin, V., Chan, T., Morrison, A. P., …
556 Kelly, A. L. (2018). Effect of 3D printing on the structure and textural properties of
557 processed cheese. *Journal of Food Engineering*, *220*, 56–64.
558 https://doi.org/10.1016/j.jfoodeng.2017.02.003
559 Lei, N., Chai, S., Xu, M., Ji, J., Mao, H., Yan, S., … Sun, B. (2020). Effect of dry heating
560 treatment on multi-levels of structure and physicochemical properties of maize starch: A
561 thermodynamic study. *International Journal of Biological Macromolecules*, *147*, 109–
562 116. https://doi.org/10.1016/j.ijbiomac.2020.01.060
563 Lille, M., Nurmela, A., Nordlund, E., Metsä-Kortelainen, S., & Sozer, N. (2018).
564 Applicability of protein and fiber-rich food materials in extrusion-based 3D printing.
565 *Journal of Food Engineering*, *220*, 20–27.
566 https://doi.org/10.1016/j.jfoodeng.2017.04.034
567 Lima, D. C., Castanha, N., Maniglia, B. C., Matta Junior, M. D., La Fuente, C. I. A., &
568 Augusto, P. E. D. (2020). Ozone Processing of Cassava Starch. *Ozone: Science &*
569 *Engineering*, 1–18. https://doi.org/10.1080/01919512.2020.1756218
570 Liu, H., Yu, L., Xie, F., & Chen, L. (2006). Gelatinization of cornstarch with different
571 amylose/amylopectin content. *Carbohydrate Polymers*, *65*(3), 357–363.
572 https://doi.org/10.1016/j.carbpol.2006.01.026
573 Liu, K., Hao, Y., Chen, Y., & Gao, Q. (2019). Effects of dry heat treatment on the structure
574 and physicochemical properties of waxy potato starch. *International Journal of*
575 *Biological Macromolecules*, *132*, 1044–1050.
576 https://doi.org/10.1016/j.ijbiomac.2019.03.146
577 Liu, Y., Liang, X., Saeed, A., Lan, W., & Qin, W. (2019). Properties of 3D printed dough and
578 optimization of printing parameters. *Innovative Food Science & Emerging Technologies*,
579 *54*, 9–18. https://doi.org/10.1016/j.ifset.2019.03.008
580 Liu, Z., Bhandari, B., Prakash, S., & Zhang, M. (2018). Creation of internal structure of
581 mashed potato construct by 3D printing and its textural properties. *Food Research*
582 *International*, *111*(March), 534–543. https://doi.org/10.1016/j.foodres.2018.05.075
583 Lopez-Sanchez, P., Nijsse, J., Blonk, H. C. G., Bialek, L., Schumm, S., & Langton, M.
584 (2011). Effect of mechanical and thermal treatments on the microstructure and
585 rheological properties of carrot, broccoli and tomato dispersions. *Journal of the Science*
586 *of Food and Agriculture*, *91*(2), 207–217. https://doi.org/10.1002/jsfa.4168
587 Maniglia, B. C., Castanha, N., Le-Bail, P., Le-Bail, A., & Augusto, P. E. D. (2020). Starch
588 modification through environmentally friendly alternatives: a review. *Critical Reviews in*

Food Science and Nutrition, *0*(0), 1–24. https://doi.org/10.1080/10408398.2020.1778633

Maniglia, B. C., Lima, D. C., Matta Junior, M. D., Le-Bail, P., Le-Bail, A., & Augusto, P. E. D. (2019). Hydrogels based on ozonated cassava starch: Effect of ozone processing and gelatinization conditions on enhancing 3D-printing applications. *International Journal of Biological Macromolecules*, *138*, 1087–1097. https://doi.org/10.1016/j.ijbiomac.2019.07.124

Maniglia, B. C., Lima, D. C., Matta Junior, M. D., Le-Bail, P., Le-Bail, A., & Augusto, P. E. D. (2020). Preparation of cassava starch hydrogels for application in 3D printing using dry heating treatment (DHT): A prospective study on the effects of DHT and gelatinization conditions. *Food Research International*, *128*((accepted for publication)), 108803. https://doi.org/10.1016/j.foodres.2019.108803

Mezger, T. G. (2006). *The rheology handbook: for users of rotational and oscillatory rheometers*. Vincentz Network GmbH & Co KG.

Muscat, D., Adhikari, B., Adhikari, R., & Chaudhary, D. S. (2012). Comparative study of film forming behaviour of low and high amylose starches using glycerol and xylitol as plasticizers. *Journal of Food Engineering*, *109*(2), 189–201. https://doi.org/10.1016/j.jfoodeng.2011.10.019

Nakamura, C., Koshikawa, Y., & Seguchi, M. (2008). Increased volume of Kasutera cake (Japanese sponge cake) by dry heating of wheat flour. *Food Science and Technology Research*, *14*(5), 431.

Nara, S., & Komiya, T. (1983). Studies on the Relationship Between Water-satured State and Crystallinity by the Diffraction Method for Moistened Potato Starch. *Starch - Stärke*, *35*(12), 407–410. https://doi.org/10.1002/star.19830351202

Oh, I. K., Bae, I. Y., & Lee, H. G. (2018). Effect of dry heat treatment on physical property and in vitro starch digestibility of high amylose rice starch. *International Journal of Biological Macromolecules*, *108*, 568–575. https://doi.org/10.1016/j.ijbiomac.2017.11.180

Ozawa, M., Kato, Y., & Seguchi, M. (2009). Investigation of Dry-Heated Hard and Soft Wheat Flour. *Starch-Stärke*, *61*(7), 398–406.

Punia, S., Sandhu, K. S., Dhull, S. B., & Kaur, M. (2019). Dynamic, shear and pasting behaviour of native and octenyl succinic anhydride (OSA) modified wheat starch and their utilization in preparation of edible films. *International Journal of Biological Macromolecules*, *133*, 110–116. https://doi.org/10.1016/j.ijbiomac.2019.04.089

Seguchi, M. (2001). Oil binding ability of chlorinated and heated wheat starch granules and

their use in breadmaking and pancake baking. *Starch-Stärke*, *53*(9), 408–413.

Shevkani, K., Singh, N., Bajaj, R., & Kaur, A. (2017). Wheat starch production, structure, functionality and applications-a review. *International Journal of Food Science & Technology*, *52*(1), 38–58. https://doi.org/10.1111/ijfs.13266

Smith, R. J. (1967). Production and use of hypochlorite oxidized starches. *Starch Chemistry and Technology*, Vol. 2, pp. 620–625. New York: Academic Press.

Song, Y., & Jane, J.-L. (2000). Characterization of barley starches of waxy, normal, and high amylose varieties. *Carbohydrate Polymers*, *41*(4), 365–377. https://doi.org/10.1016/S0144-8617(99)00098-3

Tan, C., Toh, W. Y., Wong, G., & Lin, L. (2018). Extrusion-based 3D food printing – Materials and machines. *International Journal of Bioprinting*, *4*(2). https://doi.org/10.18063/ijb.v4i2.143

Ubeyitogullari, A., & Ciftci, O. N. (2016). Formation of nanoporous aerogels from wheat starch. *Carbohydrate Polymers*, *147*, 125–132.

Xiong, J., Li, Q., Shi, Z., & Ye, J. (2017). Interactions between wheat starch and cellulose derivatives in short-term retrogradation: Rheology and FTIR study. *Food Research International*, *100*, 858–863.

Yang, F., Zhang, M., Prakash, S., & Liu, Y. (2018). Physical properties of 3D printed baking dough as affected by different compositions. *Innovative Food Science & Emerging Technologies*, *49*, 202–210. https://doi.org/10.1016/j.ifset.2018.01.001

Yeh, A.-I., & Yeh, S.-L. (1992). Some Characteristics of Hydroxypropylated and Crosslinked Rice Starches. *Cereal Chemistry*, *70*(5), 596–601.

Yu, B., Ren, F., Zhao, H., Cui, B., & Liu, P. (2020). Effects of native starch and modified starches on the textural, rheological and microstructural characteristics of soybean protein gel. *International Journal of Biological Macromolecules*, *142*, 237–243.

Zou, J., Xu, M., Tian, J., & Li, B. (2019). Impact of continuous and repeated dry heating treatments on the physicochemical and structural properties of waxy corn starch. *International Journal of Biological Macromolecules*, *135*, 379–385. https://doi.org/10.1016/j.ijbiomac.2019.05.147

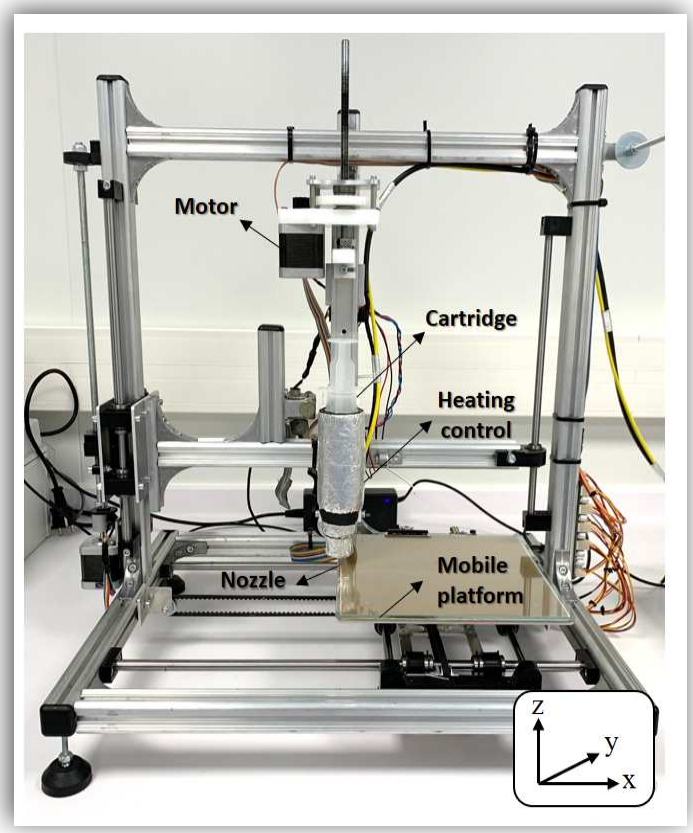

Fig. 1. The picture of 3D printer with the main parts: the extruder motor, syringe (cartridge) with the nozzle (movement in z direction), heating control, and mobile platform (movement in x and y directions).

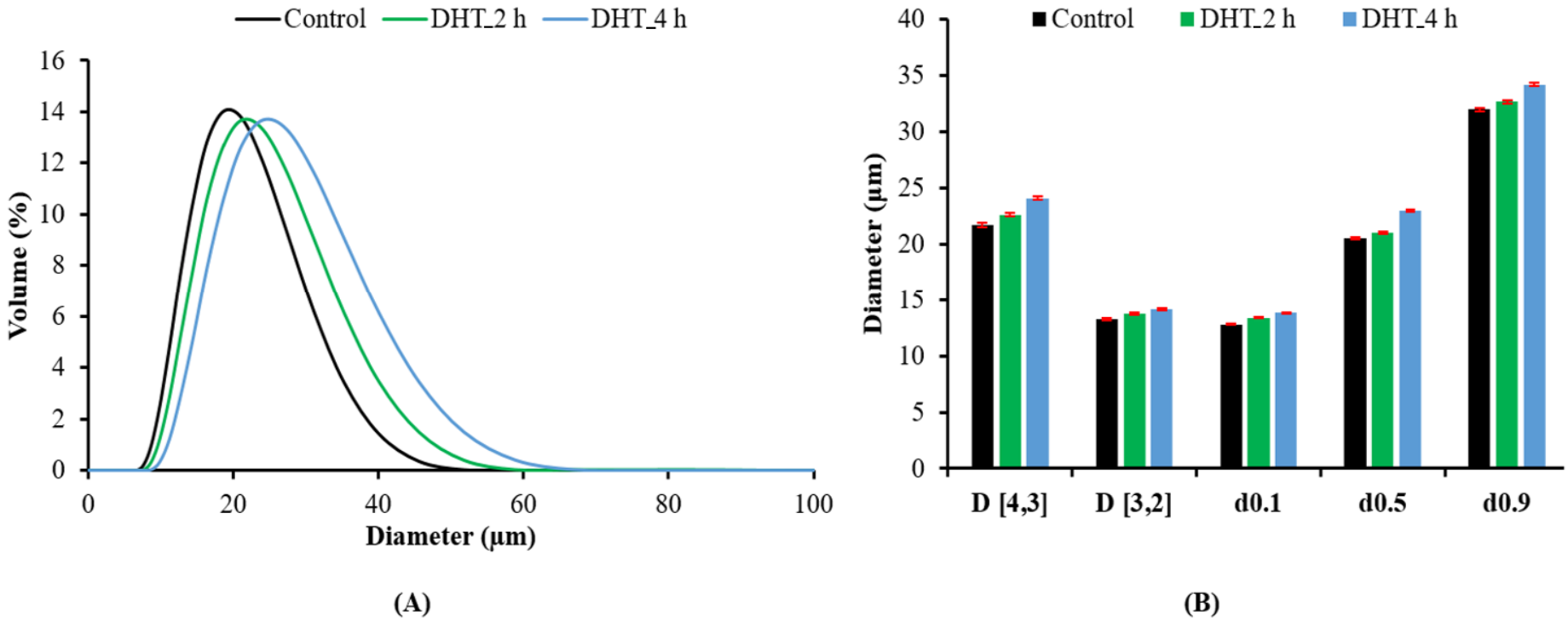

Fig. 2. (A) Granule size distribution (B) Specific diameters (D[4,3], D[3,2], d0.1, d0.5, d0.9 - vertical red bars are the standard deviation) of the control and modified starches by dry heating (DHT_2h and DHT_4h):

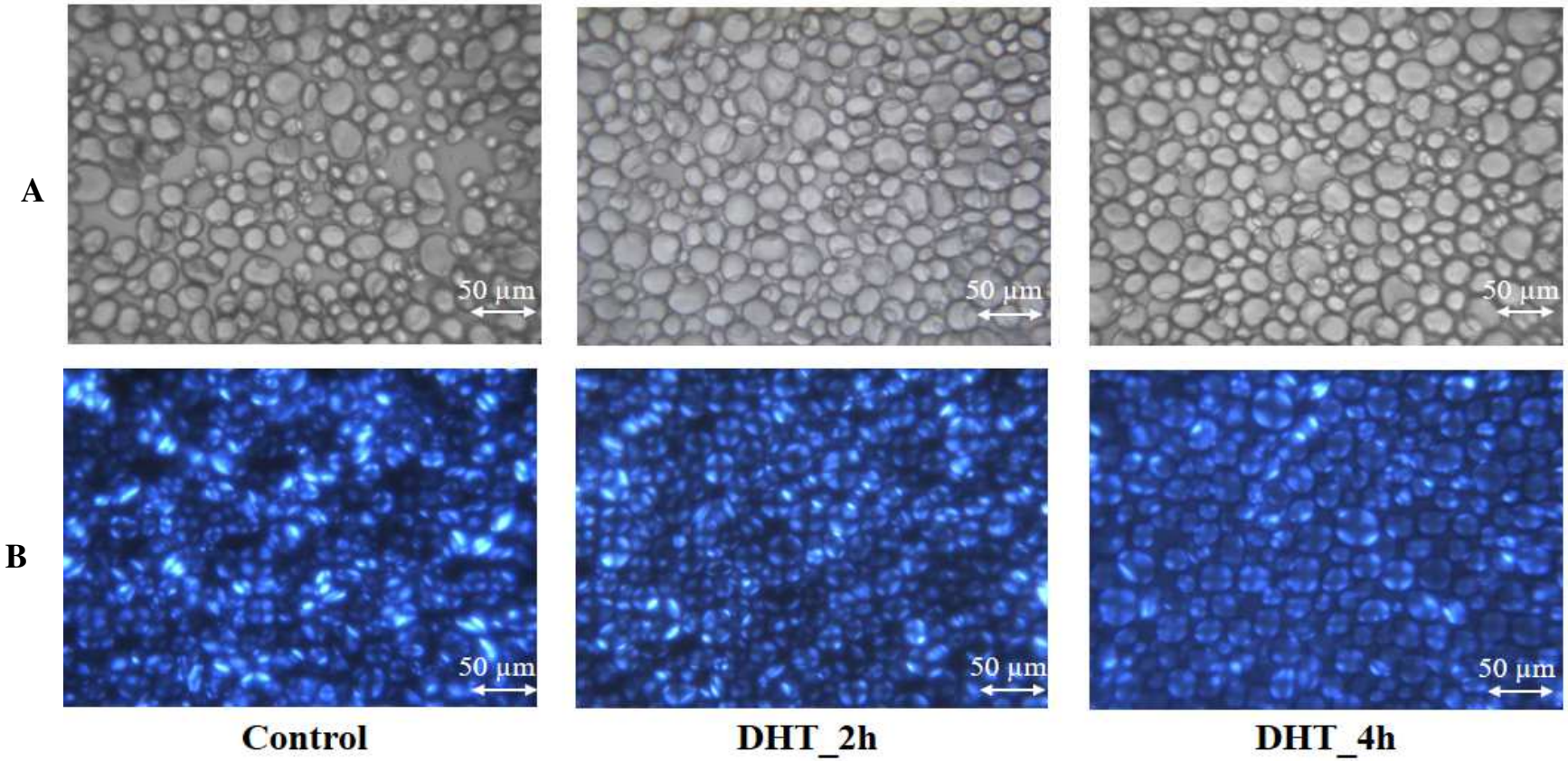

Fig. 3. Photographs from light microscopy (40×) using (A) nonpolarized and (B) polarized light of the control and modified starches by dry heating (DHT_2h and DHT_4h).

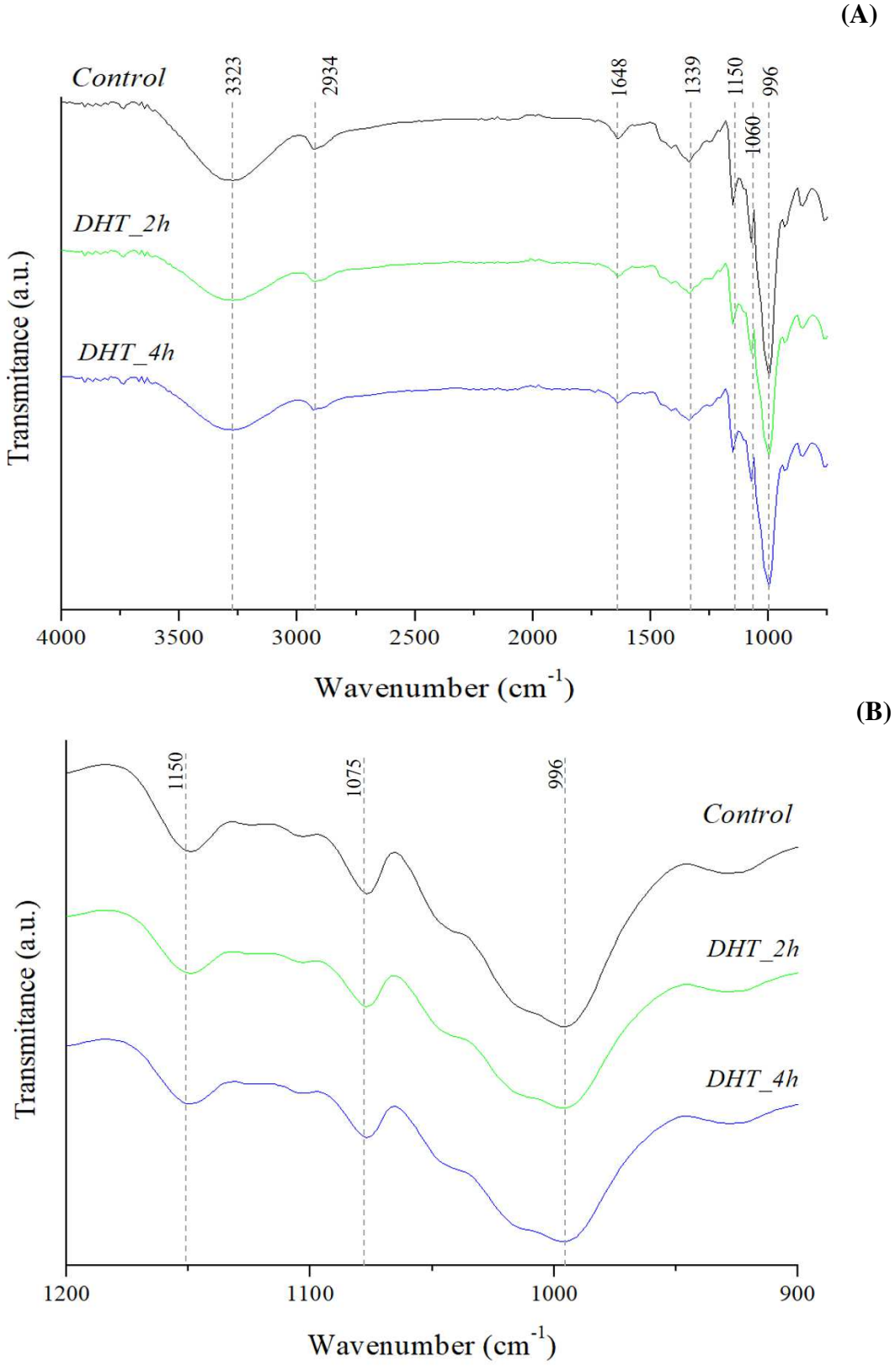

Fig. 4. (A) Vibrational spectra in wavenumber interval between (A) 4000 until 900 cm^{-1}) and between (B) 1200 until 900 cm^{-1} of the control and modified starches by dry heating treatment (DHT_2h and DHT_4h).

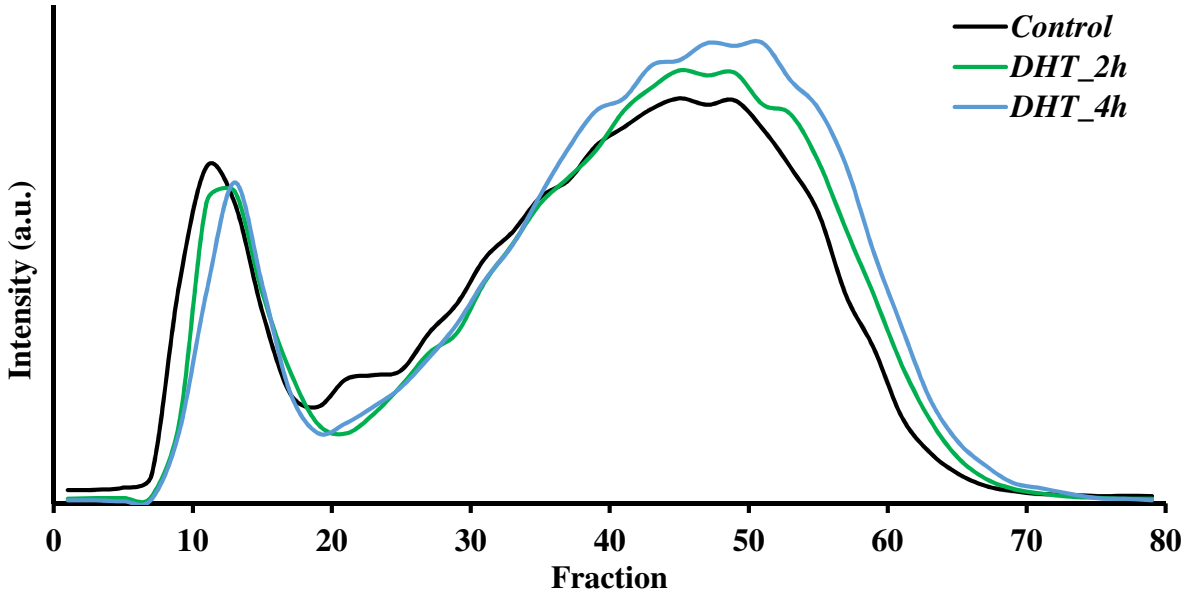

Fig. 5. Molecular size distribution of the control and modified starches by dry heating (DHT_2h and DHT_4h).

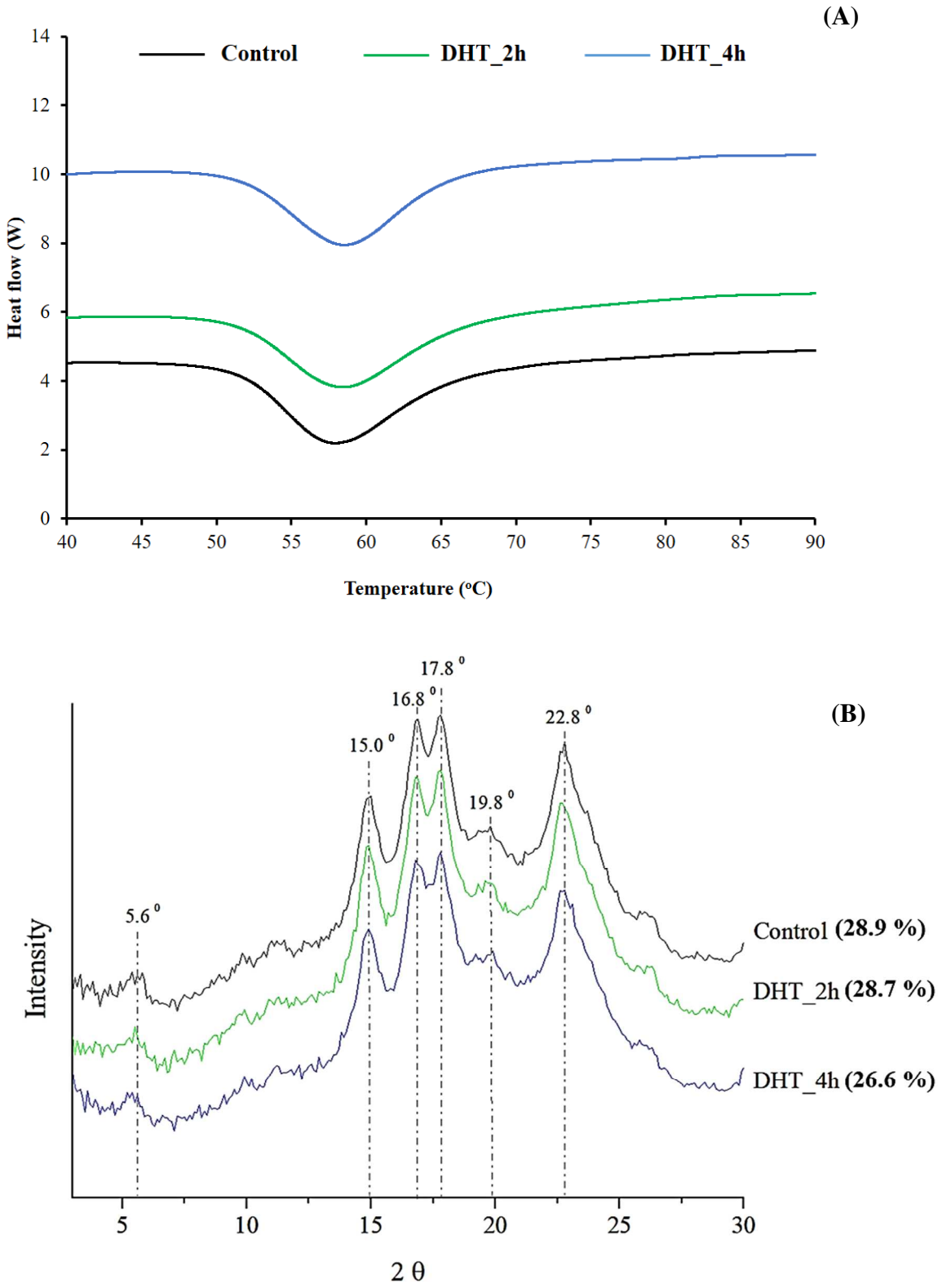

Fig. 6. (**A**) DSC thermograms and (B) XRD of control and wheat starch treated by dry heating (DHT_2 and DHT_4 h).

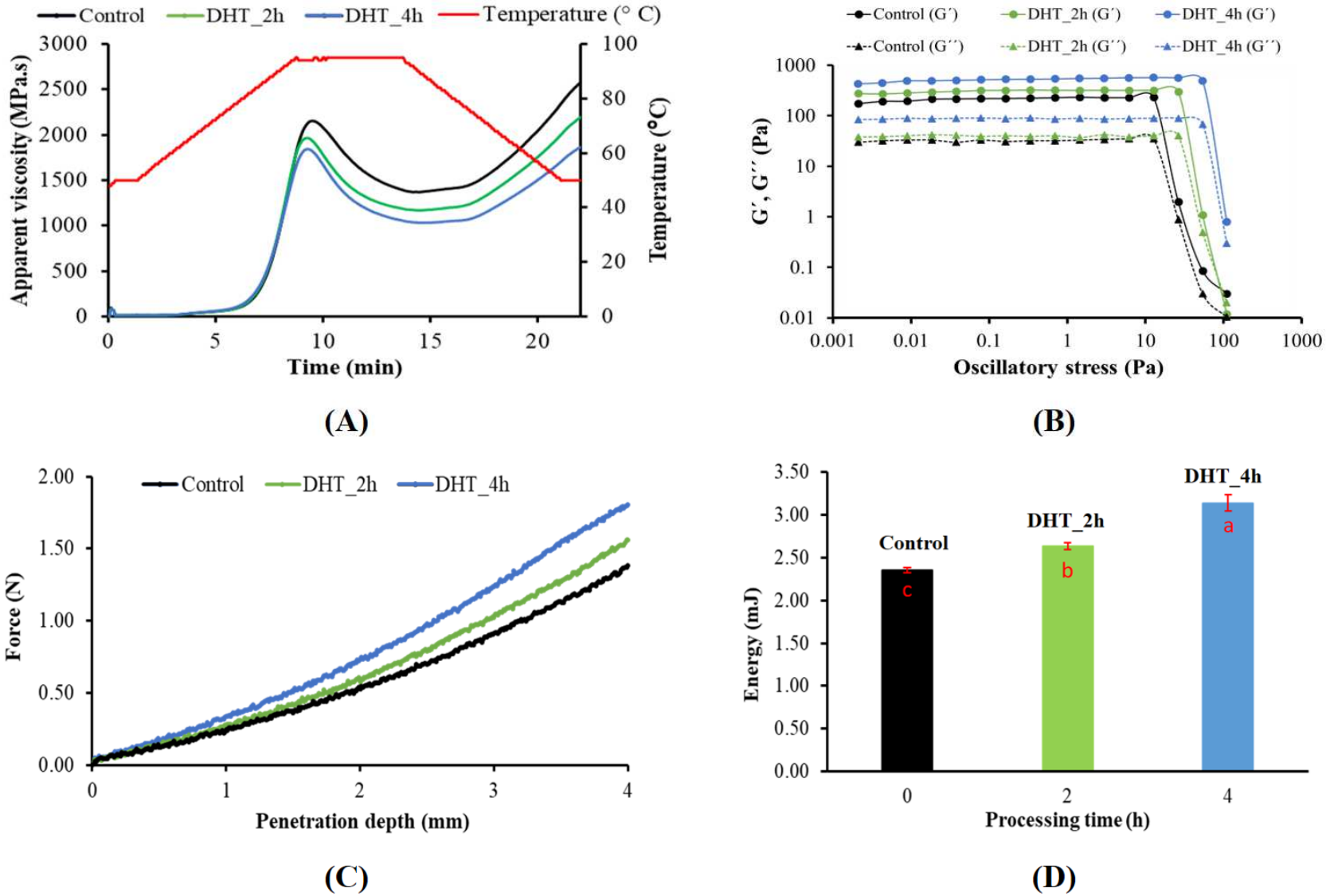

Fig. 7. (A) RVA curves, (B) oscillatory stress sweep analysis (G´: storage modulus and G´´: loss modulus), (C) Gel firmness, and (D) the energy required in a puncture assay of the control and the wheat starch treated by dry heating (DHT_2 and DHT_4 h).

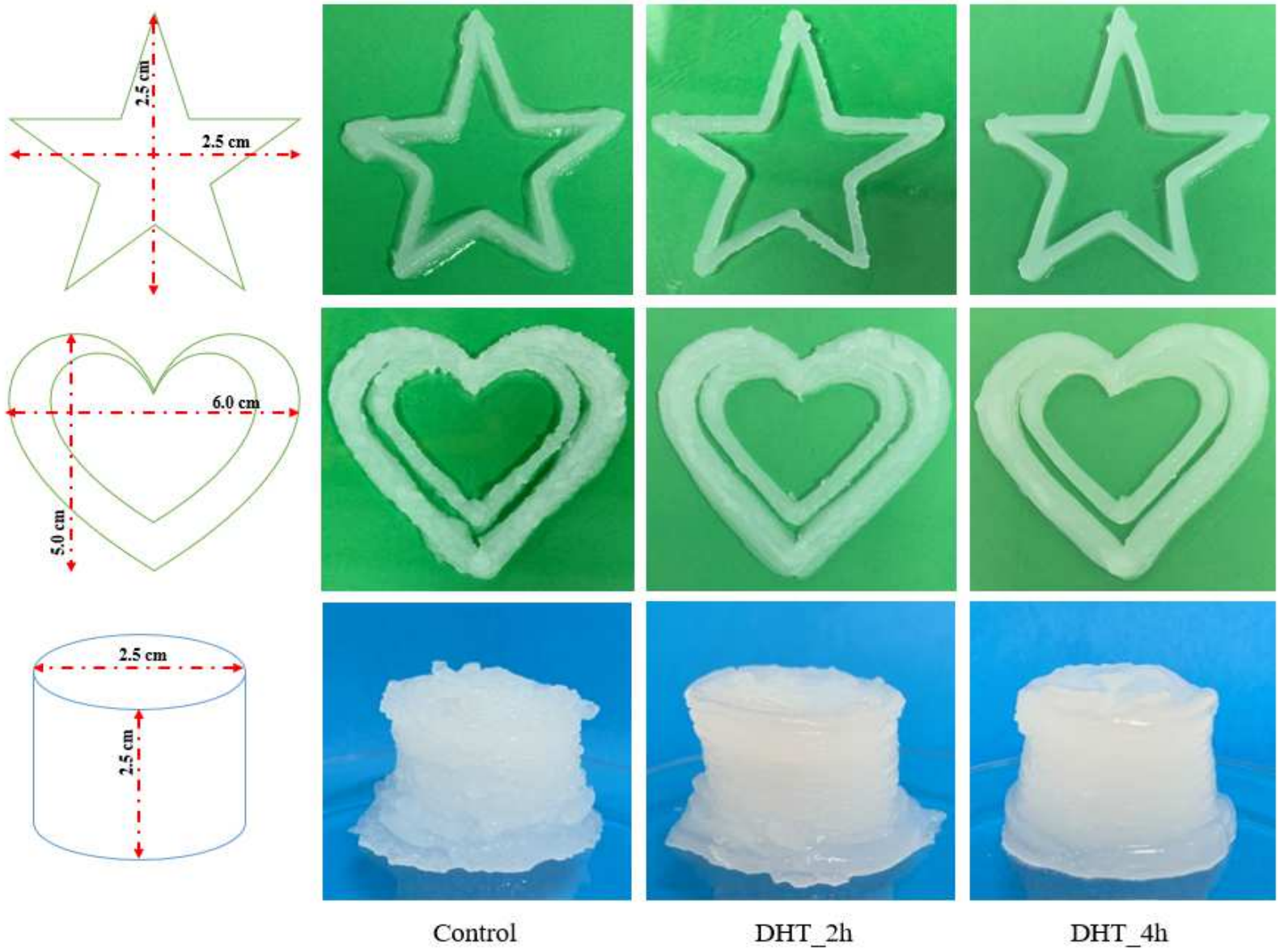

Fig. 8. The 3D printed hydrogels (star, heart, and cylindrical shapes) based on control wheat starch and modified wheat starch by dry heating treatment (DHT_2h and DHT_4h).

Table 1. Gelatinization properties of the control and modified starches by dry heating (DHT_2h and DHT_4h) (average ± standard deviation).

Samples	To (ºC)	Tp (ºC)	Tf (ºC)	ΔH (J/g)
Control	47.99 ± 0.28^{a}	58.05 ± 0.10^{c}	74.32 ± 0.56^{a}	9.85 ± 0.12^{a}
DHT_2 h	47.43 ± 0.37^{a}	58.30 ± 0.06^{b}	74.65 ± 0.62^{a}	9.89 ± 0.28^{a}
DHT_4 h	47.23 ± 0.43^{a}	59.85 ± 0.10^{a}	74.42 ± 0.35^{a}	7.57 ± 0.10^{b}

a, b, c: different letters in the same column indicates significant difference among samples, as revealed by Tukey's test, $p < 0.05$

To = onset temperature, Tp = peak temperature, Tf = final temperature and ΔH = enthalpy.

DHT_2h: wheat starch dry heating treated for 2 h. DHT_4h: wheat starch dry heating treated for 4 h.

Table 2. Pasting parameters from RVA and parameters from oscillatory stress sweep analysis of **the control and modified starches by dry heating (DHT_2h and DHT_4h)** (average ± standard deviation)

Samples	PAV (mPa.s)	TAV (mPa.s)	RBD (%)	FAV (mPa.s)	RSB (%)	PT (°C)	G´ (Pa)	G´´ (Pa)	$\sigma_{0,G'}$ (Pa)
Control	2250.40±40.92^{a}	1378.43±18.30^{a}	37.36±1.09^{c}	2757.50±14.95^{a}	40.71±0.72^{a}	73.53±0.32^{b}	175±25^{c}	33.4±2.2^{c}	12.74±0.05^{c}
DHT_2 h	2017.00±30.15^{b}	1172.80±22.30^{b}	40.45±0.82^{b}	2257.00±70.21^{b}	31.91±0.49^{b}	73.68±0.38^{b}	257±32^{b}	40.1±1.6^{b}	26.37±0.20^{b}
DHT_4 h	1820.72±22.17^{c}	1034.02±10.12^{c}	43.93±0.65^{a}	1927.50±82.73^{c}	18.73±0.42^{c}	74.53±0.25^{a}	430±14^{a}	88.9±4.5^{a}	54.56±0.08^{a}

Peak Apparent Viscosity (PAV), Through Apparent Viscosity (TAV), Relative Breakdown (RBD), Final Apparent Viscosity (FAV), Relative Setback (RSB) and Pasting Temperature (PT), Storage modulus (G'), Loss modulus (G''), Yield stress ($\sigma_{0,G'}$)

a - c: different letters in the same column indicates significant difference among samples, as revealed by Tukey's test, $p < 0.05$.

DHT_2h: wheat starch dry heating treated for 2 h. DHT_4h: wheat starch dry heating treated for 4 h.

Table 3. Texture parameters and reproducibility of the starch hydrogels printed in cylinder shape. The hydrogels are based on control and modified starches by dry heating (DHT_2h and DHT_4h) (average ± standard deviation)

Starch hydrogels	*Texture*					*Reproducibility*		
	Hardness (N)	*Adhesiveness (N.s)*	*Cohesiveness (-)*	*Springiness (-)*	*Chewiness (-)*	*Weight (g)*	*Diameter (mm)*	*Height (mm)*
Control	0.68±0.08^{c}	-1.67±0.01^{a}	0.41±0.01^{a}	0.81±0.03^{a}	0.27±0.01^{a}	15.38±0.36^{a}	2.50±0.16^{a}	2.08±0.08^{b}
DHT_2h	0.82±0.03^{b}	-2.16±0.15^{b}	0.41±0.01^{a}	0.84±0.04^{a}	0.27±0.01^{a}	14.74±0.34^{b}	2.58±0.16^{a}	2.34±0.11^{a}
DHT_4h	1.03±0.05^{a}	-2.23±0.23^{b}	0.41±0.02^{a}	0.82±0.04^{a}	0.32±0.03^{a}	14.81±0.18^{b}	2.48±0.08^{a}	2.36±0.11^{a}

a - c: different letters in the same column indicates significant difference among samples, as revealed by Tukey's test, $p < 0.05$

DHT_2h: wheat starch dry heating treated for 2 h. DHT_4h: wheat starch dry heating treated for 4 h.

DHT improved the 3D printability and extended the texture possibilities of wheat starch hydrogels

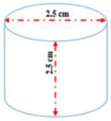

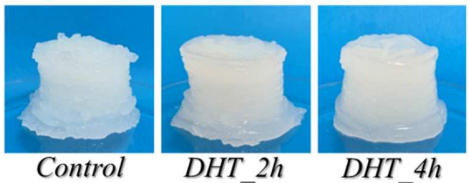

Control *DHT_2h* *DHT_4h*